# Simultaneous UV Images and Particle Measurements of an Auroral Dawn Storm at Jupiter

R. W. Ebert[1,2], T. K. Greathouse[1], G. Clark[3], F. Allegrini[1,2], F. Bagenal[4], S. J. Bolton[1], B. Bonfond[5], J. E. P. Connerney[6,7], G. R. Gladstone[1,2], V. Hue[1], M. Imai[8,9], W. S. Kurth[8], S. Levin[10], P. Louarn[11], B. H. Mauk[3], D. J. McComas[12], C. Paranicas[3], A. H. Sulaiman[8], J. R. Szalay[12], M. F. Thomsen[13], and R. J. Wilson[4]

[1]Southwest Research Institute, San Antonio, Texas, USA
[2]Department of Physics and Astronomy, University of Texas at San Antonio, San Antonio, Texas, USA
[3]Johns Hopkins University Applied Physics Lab, Laurel, Maryland, USA
[4]Laboratory for Atmospheric and Space Physics, University of Colorado Boulder, Boulder, Colorado, USA
[5]Université de Liège, Liège, Belgium
[6]Space Research Corporation, Annapolis, MD
[7]NASA Goddard Space Flight Center, Greenbelt, MD
[8]Department of Physics and Astronomy, University of Iowa, Iowa City, IA, USA
[9]Department of Electrical Engineering and Information Science, National Institute of Technology, Niihama College, Niihama, Ehime, Japan
[10]Jet Propulsion Laboratory, Pasadena, California, USA
[11]Institut de Recherche en Astrophysique et Planétologie, Toulouse, France
[12]Department of Astrophysical Sciences, Princeton University, Princeton, New Jersey, USA
[13]Planetary Science Institute, Tucson, Arizona, USA

Key Points

1. Juno observed transient UV brightening in Jupiter's dawn auroral region that rotated with the planet and had high color ratios.

2. The electrons mapping to the transient UV emissions are field-aligned and bi-directional, with energies from ~10 to 1000 keV.

3. These dawn UV emissions result from magnetospheric processes that trigger the generation of 100s of keV electrons observed at high latitude.

## Abstract

We present Juno observations between 03:00 to 06:00 UT on day-of-year 86, 2017 that link electrons in Jupiter's polar magnetosphere to images of transient, enhanced UV emissions in Jupiter's dawn auroral region known as a dawn storm. Juno ranged between 42ºN - 51ºN in magnetic latitude and 7.8 – 5.8 jovian radii during this period. The UV enhancements consist of two separate, elongated structures which extend into the nightside, rotate with the planet, move to lower latitudes over time, and have high color

ratios. The electrons mapping to these emissions exhibit sudden intensity depletions below ~10 keV coincident with intensity enhancements up to energies of ~1000 keV, consistent with the high color ratio observations. Electron pitch angle distributions are magnetic field aligned and bidirectional. These high latitude observations are a result of magnetospheric processes, likely plasma injections, that trigger the generation of 100s of keV electrons to produce these dawn emissions.

## 1. Introduction

The primary components of Jupiter's ultraviolet (UV) aurora are the main, outer, polar, and satellite emissions [see review by Grodent et al., 2015 for details]. These emissions are produced by precipitating electrons that interact with $H_2$ molecules in Jupiter's upper atmosphere [e.g. Broadfoot et al., 1979] and can be used as a diagnostic of dynamics and structure in Jupiter's magnetosphere. A number of secondary, transient UV auroral emissions have also been identified, many occurring in the dawn sector of Jupiter's auroral region [e.g. Prangé et al., 1993; Gérard et al., 1994; Ballester et al., 1996; Clarke et al., 1998; Gustin et al. 2006; Radioti et al., 2008; Kimura et al., 2015; 2017; Bonfond et al., 2020].

Clarke et al., [1998] identified bright, transient UV emissions in the local dawn region near the expected location of Jupiter's main emission. These emissions, coined 'dawn storms', showed significant spreading in longitude and remained near local dawn while other, dimmer, emissions co-rotated with the planet. Their proximity to the main emission suggested that these emissions were produced in Jupiter's middle magnetosphere. Kimura et al., [2015] interpreted these dawn storms as being driven by tail reconnection, bringing energetic particles from the outer and middle magnetosphere to the inner magnetosphere within a timeframe of < 1 – 2 planetary rotations. Gustin et al., [2006] reported on dawn UV auroral brightenings of up to ~1.8 Megarayleigh (MR), approximately 4 times brighter than the nominal main emission [Grodent et al., 2003]. These features had a leading edge that was fixed in system III longitude whereas the trailing edge seemed to be organized by local time, with an extension into the nightside of Jupiter's auroral region. UV spectral observations were used to infer the characteristic energies (up to ~50 – 500 keV), energy fluxes (5 – 90 mW $m^{-2}$) and current densities (~0.1 – 0.5 μA $m^{-2}$) of the precipitating electrons responsible for producing these emissions. These electrons were interpreted as being accelerated by electric fields in regions of upward field-aligned currents, although direct measurements of these electrons have yet to be achieved.

In July 2016, NASA's Juno mission [Bolton et al., 2017] was inserted into a 53-day polar orbit around Jupiter. Juno is a spinning spacecraft with a ~30 s spin period. Its orbit and suite of instruments provide an excellent platform to remotely image Jupiter's aurora [e.g. Connerney et al., 2017a] while simultaneously measuring *in situ* the high-latitude magnetospheric environment that map to unique auroral emissions [e.g. Ebert et al., 2019; Gérard et al., 2019]. In this letter, we present electron and UV observations associated with a transient dawn UV brightening in Jupiter's northern auroral region on day-of-year (DOY) 86, 2017, prior to Juno's 5$^{th}$ perijove (PJ5). We focus on the period from 03:00 –

05:00 UT when Juno ranged from 7.8 $R_J$ to 5.8 $R_J$ in jovicentric radial distance (1 $R_J$ = 71,492 km) and 41.6°N to 50.9°N in magnetic latitude, including an interval when the spacecraft magnetically mapped to the UV emissions under consideration here. These observations provide an opportunity to study the high latitude electron distributions that map to transient UV emissions observed in Jupiter's dawn auroral region.

## 2. Data Sets and Observing Geometry

We examine electron observations from Juno's Jovian Auroral Distributions Experiment Electron (JADE-E) sensors [McComas et al., 2017] and Jupiter Energetic particle Detector Instrument (JEDI) [Mauk et al., 2017a], magnetic field observations from the Magnetic Field Investigation (MAG) [Connerney et al., 2017b] and UV emissions from the Ultraviolet Spectrograph (UVS) [Gladstone et al., 2017]. JADE-E and JEDI measure electron fluxes in the energy range, 0.1 – 100 keV and 30 – 1000 keV, respectively, along with their pitch angle distributions, with a time resolution down to 1 s. MAG consists of two independent sensor suites, each containing a tri-axial fluxgate magnetometer (FGM) and a pair of imaging sensors. The FGMs simultaneously measure the magnetic field at a rate of 64 vector samples per second. We utilize 1 s magnetic field vector observations from MAG to calculate the electron pitch angle distributions. UVS is an imaging spectrograph sensitive to wavelengths between 68 and 210 nm. It observes Jupiter's northern and southern auroras for several hours bounding each Juno perijove pass from jovicentric distances of ~1.3 – 7 $R_J$. A scan mirror allows the field-of-view (FOV) to be directed ±30° relative to Juno's spin plane giving UVS access to half the sky at any given spacecraft orientation. The UV brightness is determined by integrating the emissions between 115 – 118 nm and 125 – 165 nm and then multiplying by 1.84 to estimate the total $H_2$ emission between 75 – 198 nm. See the instrument papers cited above for more details.

Figure 1 shows Juno's trajectory on approach to PJ5 and projected onto Jupiter's atmosphere in a magnetic coordinate system based on the JRM09 internal magnetic field [Connerney et al., 2018] and the magnetodisc model of Connerney et al., [1981], where $Z_{MAG}$ is along Jupiter's magnetic dipole axis. M, or M-shell, corresponds to a distance based on the predicted magnetic equator crossing distance for any given magnetic field line. Juno's magnetic footpoint maps along Jupiter's northern main auroral oval from ~2:00 – 6:30 UT on DOY 086, 2017. The periods of interest are highlighted by the thick red, blue, and green lines. The blue line corresponds to an interval when Juno made *in situ* measurements of plasma, energetic particles, and fields while simultaneously observing bright UV features near Jupiter's main emission.

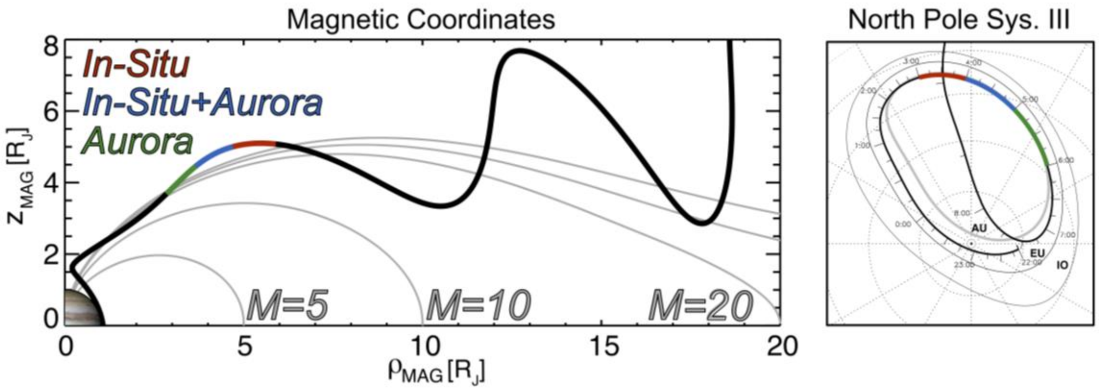


**Figure 1**: *(Left) Juno's inbound trajectory (black line) in Jupiter's northern hemisphere prior to perijove 5 on days-of-year 85 – 86, 2017. The trajectory is shown in a magnetic coordinate system [Connerney et al., 1981; 2018]. Magnetic field lines, and the M-shells that they map to, are shown in grey. (Right) Magnetic projection of Juno's trajectory onto Jupiter's upper atmosphere. Black dashed circles and lines are contours of constant jovicentric latitude and system III longitude, respectively. Thick grey oval (AU) denotes the statistical average position of Jupiter's main ultraviolet (UV) aurora [Bonfond et al., 2012]. Thin grey ovals identify the location of the Io and Europa auroral footprints. Thick red, blue, and green lines highlight the periods of interest.*

## 3. UV Aurora and High-Latitude Magnetosphere Observations

Figure 2 presents UV brightness (left column) and color ratio (right column) maps of Jupiter's northern auroral region covering the period from 3:58 – 6:06 UT on DOY 86, 2017. Each map is a composite of 12 different images obtained over a ~6-minute interval, each image having ~17 ms of integration time. The color ratio, defined as the ratio between the integrated brightness from 158 to 162 nm and 126 to 130 nm, is used to estimate the depth from which the UV emissions are generated and the characteristic energy of the precipitating electrons that produce them. A larger color ratio is interpreted as representing more energetic electrons that produce the UV emissions [Gérard and Singh, 1982].

This study focuses on the bright UV emissions observed on the left side of Figure 2(a), near the statistical average latitude of the main aurora, denoted by the white dashed ovals [Bonfond et al., 2012]. These UV emissions consist of two bright, elongated features on the dawn side of the auroral region, a leading spot near the terminator, and a trailing spot on the nightside. Figures 2(b) – 2(e) are a time series of the auroral images and show that these features rotate with the planet. The emissions also show a slight displacement to lower latitude over time, an indication that the driver of the feature is moving radially inward toward Jupiter. The leading and trailing emissions have a mean brightness of 600 ± 210 and 730 ± 280 kilorayleighs (kR), respectively, throughout the interval considered here. The brightness and extent of these features vary with time, the brightness of the leading spot dimming to ~500 and 450 kR, respectively, in Figures 2(d) and 2(e).

The image in Figure 2(f) indicates that the UV features under consideration have relatively high color ratios, between ~ 10 – 20, compared to the surrounding emissions.

The color ratio for the nightside emission is greater than for the emission near the terminator, suggesting that the nightside emissions are produced by more energetic electrons. Figures 2(g) – 2(i) show that the color ratio for the leading emission feature is reduced as it rotates towards the dayside while the color ratio for the trailing emission feature remains relatively higher throughout the interval.

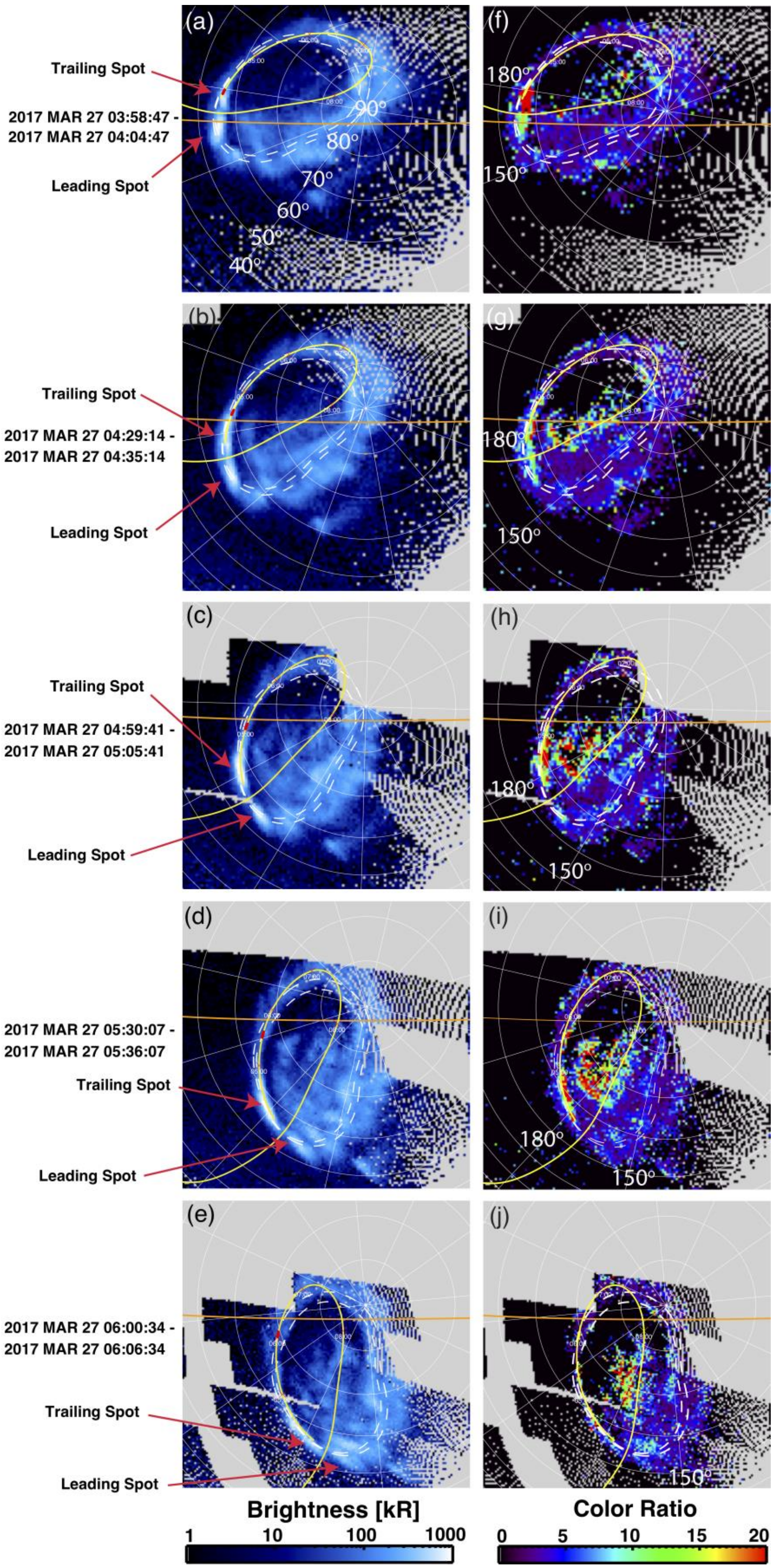
(a)
(f)
(b)
(g)
(c)
(h)
(d)
(i)
(e)
(j)
Trailing Spot
Leading Spot
2017 MAR 27 03:58:47 -
2017 MAR 27 04:04:47
2017 MAR 27 04:29:14 -
2017 MAR 27 04:35:14
2017 MAR 27 04:59:41 -
2017 MAR 27 05:05:41
2017 MAR 27 05:30:07 -
2017 MAR 27 05:36:07
2017 MAR 27 06:00:34 -
2017 MAR 27 06:06:34
90°
80°
70°
60°
50°
40°
180°
150°
Brightness [kR]
1
10
100
1000
Color Ratio
0
5
10
15
20

173

**Figure 2**: *(a) – (e) Ultraviolet (UV) brightness images in Jupiter's northern auroral region on day-of-year 086, 2017 from 03:58 to 06:06 UT. (f) – (j) Color ratio images for the same intervals as shown for the UV brightness. These images are shown in chronological order. Red arrows in (a) – (e) point to the emissions studied here. Yellow lines identify Juno's trajectory. Orange lines denote the day-night terminator, the Sun direction being the bottom of each image. The two white dashed lines represent the statistical average compressed and expanded position of Jupiter's main ultraviolet (UV) aurora [Bonfond et al., 2012].*

Figure 3 presents UV aurora and polar magnetosphere electron observations from DOY 086, 2017. The UV brightness (Figure 3a) and color ratio (Figure 3b) images were obtained from observations collected between 03:58 and 04:04 UT, when Juno's magnetic footprint mapped to the auroral features highlighted in the fuchsia box. The magnetospheric observations (Figures 3c – 3e) cover the time range from 03:00 – 05:00 UT. During this timeframe, Juno moved inward toward Jupiter from 7.8 to 5.8 $R_J$ and to higher northern magnetic latitudes, 42°N to 51°N. The vertical fuchsia rectangular box highlights electron observations that coincide with the auroral observations in Figures 3a and 3b.

Figures 3(c) shows an energy versus time spectrogram of differential energy flux for 0.1 – 1000 keV electrons based on combined JEDI and JADE-E observations. The JEDI observations (> 100 keV) have a 1 s time resolution throughout this period while the JADE-E observations have a resolution of 1 s from 03:00 –03:30 UT and a 30 s resolution from 03:30 – 05:00 UT. The transition between the JADE and JEDI data presented here is at 100 keV. At times, the differential energy fluxes show a notable discontinuity when transitioning from JADE to JEDI energies. This could be due to a difference in calibration factors between these instruments or to their different fields-of-view, angular resolution and/or energy resolution [Allegrini et al., 2020].The electron distributions show variations in both differential energy flux and energy. The most notable features are the depletions in low-energy electrons observed between ~03:11 – 03:12, 3:18 – 03:26, and 03:53 – 04:25 UT. During these times, the minimum energy of the electrons increases from < ~200 eV to ≥ 10 keV, the bulk of their differential energy flux distributions being at energies > 100 keV, with their maximum energy exceeding 500 keV. A closer inspection of the JEDI data from ~03:18 – 03:26 and 04:00 – 04:15 UT shows the presence of penetrating electrons (> 1 MeV), identified by an enhanced horizontal band just above 160 keV in the electron energy spectrogram. The interval between 03:53 – 04:25 UT contains the period where the electrons map to the dawn UV emissions highlighted in Figures 3(a) and 3(b), the increase in electron energy being consistent with the high UV color ratio observations.

The pitch angle distributions for the ~30 keV – 1 MeV electrons in Figure 3(d) are primarily between 0 - 30° and 150 - 180°, indicating that the electrons are field-aligned and bi-directional, traveling both towards (downward) and away (upward) from Jupiter. The pitch angles for the 0.1 – 100 keV electrons between 03:00 – 03:30 UT in Figure 3(e) are also primarily field-aligned and bi-directional, both during times when the low-energy electrons are prominent and when they are depleted. The pixels colored in black denote pitch angles that are not sampled. After 03:30 UT, JADE-E is in 30 s low rate science mode and the < 100 keV electrons observed during this period also show field-aligned and bi-directional distributions. The loss cone at Juno's radial distance during this timeframe ranged from ~4° - 2.5°, which is below the pitch angle resolution for JEDI and JADE.

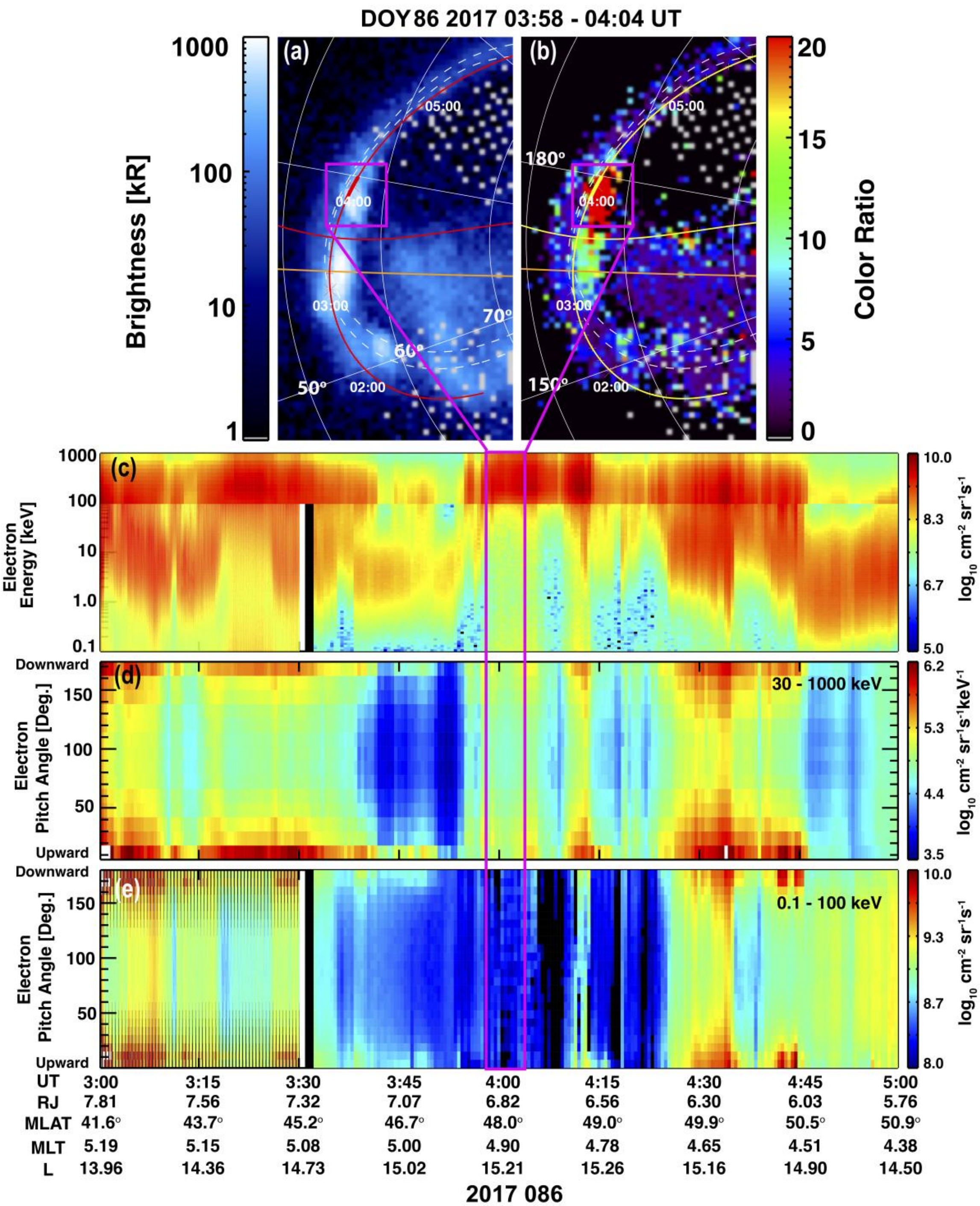

**Figure 3**: *(a) and (b) UV brightness and color ratio images from 03:58 – 04:04 UT on DOY 86, 2017. Data gaps are denoted by grey pixels. (c) Energy versus time differential energy flux spectrograms for 0.1– 1000 keV electrons. (d) and (e) Electron pitch angle distributions for 30 – 1000 keV and 0.1 – 100 keV electrons, respectively. The fuchsia boxes identify the UV emission and color ratio features that Juno is mapping to and the corresponding magnetospheric observations.*

Figure 4 combines JADE-E and JEDI observations to examine the differential intensity versus energy and pitch angle distributions of 0.1 – 1000 keV electrons from 03:58 – 04:04 UT on DOY 086, 2017. The electron intensities are averaged over this interval. These electron distributions are expected to map and contribute to the simultaneously observed UV emissions highlighted by the fuchsia boxes in Figures 3(a) and 3(b). The other intervals mentioned above which contain enhancements in 100s of keV electron intensities are likely also contributing to the two bright UV features described in this study. The intensity versus energy distribution in Figure 4 (left) shows a decreasing power law profile to at least ~ 20 keV and a slight increase between ~20 – 100 keV, which may be due to residual background signal incompletely removed from the observations. Potential causes for disagreement between JADE and JEDI intensities at overlapping energies are described above and detailed in Allegrini et al., [2020]. The distinct bump in intensities between ~150 – 500 keV is likely due to a JEDI instrument artifact where energetic electrons (> ~ 750 keV) pass through the solid state detectors and produce a signal in this energy range. It is a signature that high energy (> ~750 keV) electrons are present in the distribution [see Mauk et al., 2018 for details]. The electron intensity enhancements extend up to at least 1000 keV. Due to these different instrument effects, caution should be exercised when interpreting these intensity values. The pitch angle distributions for the 1 – 10 keV and 10 – 100 keV electrons are relatively flat, while the 30 – 1000 keV electrons have intensity enhancements between pitch angles of ~0° – 30° and 150 – 180° and a depression centered on 90°. Electrons with pitch angles near 0° and 180° are moving away from (upward) and toward (downward) Jupiter, respectively, along the magnetic field.

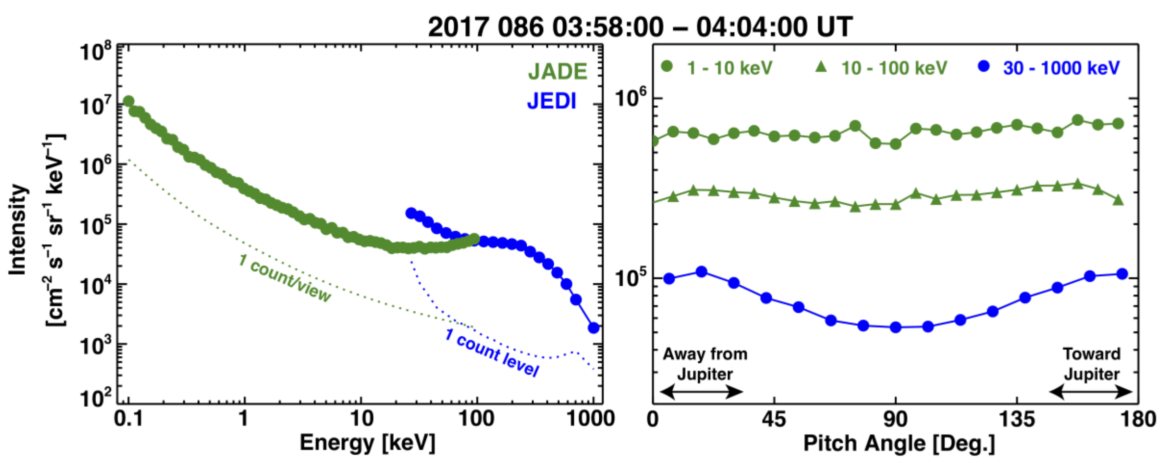


**Figure 4**: (Left) Intensity versus energy for ~0.1 – 1000 keV electrons mapping to the dawn UV emissions highlighted in Figure 3(a) and 3(b). The green dotted line represents the intensity generated by 1-count per view in the JADE-E level-2 data. The blue dotted

line identifies the 1-count level intensity in the JEDI data (Right) Intensity versus pitch angle for ~1 – 1000 keV electrons from the same interval. Pitch angles associated with electrons moving away from (upward) and toward (downward) Jupiter are identified.

## 3. Discussion

We present *in situ* and remote sensing observations from Juno that connect electrons in Jupiter's polar magnetosphere to transient UV auroral brightenings near Jupiter's northern main auroral oval. The transient UV emissions, consisting of two separate, elongated structures with high color ratios, were observed in the dawn auroral region, extended into the nightside, rotated to the dayside, and showed a displacement to lower latitude, suggesting that the process initiating the generation of these UV emissions was in the middle magnetosphere [e.g. Clarke et al., 1998], moving in the direction of Jupiter's rotation and towards the planet.

These UV emissions have similar characteristics as the UV brightenings described by Gustin et al., [2006] (high color ratios, leading edge corotating with the planet, trailing edge extending into the nightside) and have features that are often attributed to dawn storms. According to Bonfond et al., [2020], dawn storms originate near midnight and are initially fixed in magnetic local time. The UV emissions then brighten, their color ratios increasing, as they move towards dawn and are observed to corotate with the planet. Kimura et al., [2017] noted that after onset, dawn storms expand in latitude and longitude, have a rapid increase in total UV power, and produce emissions equatorward of the main auroral oval, during the peak phase of the storm. The UV emissions presented here are consistent with several of these dawn storm features. The UV brightness of this dawn storm was below 1 MR and showed considerable dimming as it rotated to Jupiter's dayside, suggesting that it was a comparatively weak event.

The electrons mapping to these transient UV features range from ~10 to 1000 keV and provide further evidence that dawn storms are produced by energetic, 100s of keV, electrons. This is consistent with the high color ratio observations for this event and the long-standing interpretation based on electron energy estimates derived from color ratios of remotely sensed UV emissions from Jupiter's auroral region [e.g. Gustin et al., 2006]. Though, since neither JADE or JEDI can resolve the loss cone at the radial distance of the observations, we cannot make definitive statements about the electron distributions that are precipitating into the atmosphere to produce these dawn storm emissions at this time.

The electron differential energy flux distributions measured *in situ* show several distinct characteristics. At times, the bulk of the electrons reside between ~1 – 100 keV and extend to as low as ~100 – 200 eV. We interpret these observations as plasma sheet electrons that have migrated along magnetic field lines to higher latitudes, but have not been subjected to additional acceleration. During other times, the electron distributions are depleted at energies below < 10 keV and enhanced at energies of 100s keV. These distributions reflect a hot population of electrons that have been energized. That these hotter and colder electron populations are interspersed likely reflect a large-scale dynamic process in Jupiter's magnetosphere at this time.

One candidate is plasma injections [e.g. Mauk et al., 1997], where hot, tenuous plasma is radially transported planetward while cold, dense plasma is transported outward [e.g. Dumont et al., 2014]. Plasma injections are thought to be produced by processes related to interchange instability [Thorne et al., 1997; Mauk et al., 1999] and/or tail reconnection [e.g. Krupp et al., 1998; Louarn et al., 2014; Gray et al., 2016; Kimura et al., 2017]. Mauk et al., [2002] proposed two mechanisms for how plasma injections can produce auroral emissions at Jupiter. The first is electron scattering by magnetospheric waves that modifies the electron pitch angle distribution into a more field-aligned configuration. Recent simulations by Dumont et al., [2018] have suggested that electron pitch angle scattering by whistler mode waves could reproduce the auroral signatures associated with plasma injections. The second mechanism involves current flows along the boundary of the high-pressure region of injected plasma, where field-aligned currents travel towards and away from Jupiter. These currents interact with plasma near the planet to produce downward accelerated electrons and auroral emissions that map to the trailing edge of the injected hot plasma distribution that's rotating with Jupiter. The electron distributions associated with the dawn storm emissions studied here were energetic (100s of keV), field-aligned, and bi-directional at Juno's location (6 – 8 $R_J$ from Jupiter, 40 – 50°N magnetic latitude, L = 14 – 15), meaning that currents were flowing both towards and away from Jupiter. These observations are more consistent with the second mechanism being the driver of these emissions. It also provides important constraints for the first mechanism: that the wave-particle interactions must generate bi-directional, field-aligned beams and that these beams are generated between the equatorial and polar magnetosphere, at a significant distance (at least 6 – 8 $R_J$) from the planet.

The intensity-energy distributions of the electrons mapping to the dawn storm emissions had a power-law profile up to at least 20 keV, and extended up to 1000 keV. Broad energy distributions are a signature of stochastic particle acceleration (as opposed to acceleration by electrostatic potentials which show a mono-energetic peak in the intensity-energy distributions). Stochastic acceleration appears to be significant in energizing electrons that produce UV emissions associated with Jupiter's diffuse [Li et al. 2017], main [Mauk et al. 2017, 2020, Allegrini et al. 2017, 2020], polar [Ebert et al. 2017, 2019], and satellite footprint [Szalay et al. 2018, 2020] aurora. Proposed mechanisms include dissipation of turbulent Alfvénic fluctuations [Saur et al. 2003], resonance with whistler waves [Kurth et al. 2018, Elliott et al. 2018], electron Landau damping of kinetic Alfvén waves [Saur et al. 2018], and incompressible magnetic [Alfvénic] turbulence [Gershman et al. 2019]. Electron observations mapping to dawn storm emissions at radial distances where the loss cone can be resolved by JADE and JEDI are required to determine whether stochastic processes are responsible for accelerating the electrons that produce dawn storms.

**Acknowledgements**

This work was supported as a part of the work on the Jovian Auroral Distributions Experiment (JADE) and Juno Ultraviolet Spectrograph (Juno UVS) on NASA's Juno mission. The Jovian Energetic particle Detector Instrument (JEDI) work was funded by NASA's New Frontiers Program for Juno via a subcontract with the Southwest Research Institute. The research at the University of Iowa was supported by NASA through Contract 699041X with the Southwest Research Institute. The JNO-J/SW-JAD-3-CALIBRATED-V1.0, JNO-J-UVS-3-RDR-V1.0, JNO-J-JED-3-CDR-V1.0, and JNO-J-3-FGM-CAL-V1.0 data sets used in this study can be obtained from the Planetary Data System (PDS) at this site (**https://pds.nasa.gov/**).

**References**

Allegrini, F., et al. (2017), Electron beams and loss cones in the auroral regions of Jupiter, *Geophys. Res. Lett.*, doi:10.1002/2017GL073180.

Allegrini, F. et al. (2020), Energy flux and characteristic energy of electrons over Jupiter's main auroral emission, *J. Geophys. Res.*, doi:10.1029/2019JA027693.

Ballester, G. E. et al. (1996), Time-resolved observations of Jupiter's far-ultraviolet aurora, *Science*, 274, 5286, 409 – 413.

Bolton, S. J., Lunine, J. Stevenson, D., Connerney, J. E. P., Levin, S., et al. (2017), The Juno mission, Space Sci Rev., 213, 1 – 4, p. 5-37.

Bonfond, B., et al. (2012), Auroral evidence of Io's control over the magnetosphere of Jupiter, *Geophys. Res. Lett.*, 39, 348 L01105, doi:10.1029/2011GL050253.

Bonfond, B. et al. (2020), Substorm-like aurora at Jupiter,https:/doi.org/10.1002/essoar.10502511.1

Broadfoot, A. L. et al. (1979), Extreme Ultraviolet Observations from Voyager 1 Encounter with Jupiter, *Science*, 204, 4396, 979 – 982.

Clarke, J. T. et al. (1998), Hubble Space Telescope imaging of Jupiter's UV aurora during the Galileo orbiter mission, *J. Geophys. Res.*, 103, E9, 20217 – 20236.

Connerney, J. E. P., M. H. Acuna, and N. F. Ness (1981), Modeling the Jovian current sheet and inner magnetosphere, *J. Geophys. Res.*, 86, 8370–8384.

Connerney, J. E. P., et al. (2017a). Jupiter's magnetosphere and aurorae observed by the Juno spacecraft during its first polar orbits, *Science*, *356*(6340), 826 – 832. https://doi.org/10.1126/science.aam5928

Connerney, J. E. P., et al. (2017b) The Juno Magnetic Field Investigation, *Space Sci. Rev.*, 213, 1 – 4, doi: 10.1007/s11214-017-0334-z.

Connerney, J. E. P., Kotsiaros, S., Oliversen, R. J., Espley, J. R., Joergensen, J. L., et al. (2018), A new model of Jupiter's magnetic field from Juno's first nine orbits, Geophys. Res. Lett., 45, 6, 2590 – 2596.

Dumont, M., D. Grodent, A. Radiotti, B. Bonfond, and J.-C. Gérard (2014), Jupiter's equatorward auroral features: Possible signatures of magnetospheric injections, J. Geophys. Res., 119, 10,068 – 10,077, doi: 10.1029/2018JA025708.

Dumont, M. et al., (2018), Evolution of the auroral signatures of Jupiter's magnetosphere injections, *J. Geophys. Res.*, 123, 8489 – 8501.

Ebert, R. W., et al. (2017), Spatial distribution and properties of 0.1 – 100 keV electrons in Jupiter's polar aurora region, *Geophys. Res. Lett.*, *44*, 18, 9199 – 9207, doi://10.1002/2017GL075106.

Ebert, R. W. et al. (2019), Comparing electron energetics and UV brightness in Jupiter's northern polar auroral region prior for Juno perijove 5, *Geophys. Res. Lett.*, 46(1), 19 – 27, doi: 10.1029/2018GL081129.

Gérard, J.-Cl. and V. Singh (1982), A model of energy deposition of energetic electrons and EUV emission in the Jovian and Saturnian atmospheres and implications, J. Geophys. Res., 87, A6, 4524 – 4532.

Gérard, J.-C. et al. (1994), A remarkable auroral event on Jupiter observed in the ultraviolet with the Hubble Space Telescope, *Science*, 266, 1675 – 1678..

Gérard, J.-C., B. Bonfond, B. Mauk, G.R. Gladstone, Z.H. Yao, T.K. Greathouse, et al. (2019). Contemporaneous observations of Jovian energetic auroral electrons and ultraviolet emissions by the Juno spacecraft. Journal of Geophysical Research: Space Physics, *J. Geophys. Res.: Space Physics*, 124. https://doi.org/10.1029/2019JA026862

Gershman, D. J., Connerney, J. E. P., Kotsiaros, S., DiBraccio, G. A., Martos, Y. M., F.-Viñas, A., et al (2019). Alfvénic fluctuations associated with Jupiter's auroral emissions. *Geophys. Res. Lett.*, 46. https://doi.org/10.1029/2019GL082951

Gladstone, G. R., et al. (2017), The ultraviolet spectrograph on NASA's Juno mission, *Space Sci. Rev.*, 213, 1 – 4, doi:10.1007/s11214-014-0040-z.

Grodent, D., et al. (2003), Jupiter's polar aurora emissions, *J. Geophys. Res.*, 108, A10, SMP 6-1, CiteID 1366, DOI 10.1029/2003JA010017.

Grodent, D., (2015), A brief review of ultraviolet auroral emissions on giant planets, *Space Sci. Rev.*, 187, 23 – 50.

Gustin, J., S. W. H. Cowley, J.-C. Gérard, G. R. Gladstone, D. Grodent, and J. T. Clarke (2006), Characteristics of jovian morning bright FUV aurora form Hubble Space

Telescope/space telescope imaging spectrograph imaging and spectral observations, *J. Geophys. Res.*, 111, A09220.

Kimura, T. et al. (2015), Transient internally driven aurora at Jupiter discovered by Hisaki and the Hubble Space Telescope, *Geophys. Res. Lett.*, 42, 1662 – 1668.

Kimura et al. (2017), Transient brightening of Jupiter's aurora observed by the Hisaki satellite and Hubble Space Telescope during approach phase of the Juno spacecraft, *Geophys. Res. Lett.*, 44, 4523 – 4531.

Krupp, N., J. Woch, A. Lagg, B. Wilken, S. Livi, and D. J. Williams (1998), Energetic particle bursts in the predawn jovian magnetotail, *Geophys. Res. Lett.*, 25(8), 1249 – 1252.

Kurth, W. S., Mauk, B. H., Elliott, S. S., Gurnett, D. A., Hospodarsky, G. B., Santolik, O., et al. (2018). Whistler mode waves associated with broadband auroral electron precipitation at Jupiter. Geophysical Research Letters, 45. https://doi.org/10.1029/2018GL078566

Li, W. et al. (2017), Understanding the origin of Jupiter's diffuse aurora using Juno's first perijove observations, *Geophys. Res. Lett.*, 44, 10,162–10,170. https://doi.org/10.1002/2017GL075545

Mauk, B. H., D. J. Williams, and R. W. McEntire (1997), Energy-time dispersed charged particle signatures of dynamic injections in Jupiter's inner magnetosphere, *Geophys. Res. Lett.*, 24(23), 2949 – 2952.

Mauk, B. H., D. J. Williams, R. W. McEntire, K. K. Khurana, and J. G. Roederer (1999), Storm-like dynamics of Jupiter's inner and middle magnetosphere, *J. Geophys. Res.*, 104 (A10), 22,759 – 22,778.

Mauk, B. H, J. T. Clarke, D. Grodent, J. H. Jr. Waite, C. P. Paranicas, and D. J. Williams (2002), Transient aurora on Jupiter from injection of magnetospheric electrons, Nature, 415, 1003 – 1005.

Mauk, B. H., et al. (2017a), The Jupiter energetic particle detector instrument (JEDI) investigation for the Juno mission, *Space Sci. Rev.*, doi:10.1007/s11214-013-0025-3.

Mauk, B. H. et al. (2017b), Juno observations of energetic charged particles over Jupiter's polar regions: Analysis of mono- and bi-directional electron beams, *Geophys. Res. Lett.*, 44, doi:10.1002/2016GL072286.

Mauk, B. H. et al. (2020), Energetic particles and acceleration regions over Jupiter's polar cap and main aurora; a broad overview, *J. Geophys. Res.*, **https://doi.org/10.1029/2019JA027699**

McComas, D. J., et al. (2017), The Jovian auroral distributions experiment (JADE) on the Juno mission to Jupiter, Space Sci. Rev., 213, 1 – 4, doi: 10.1007/s11214-013-9990-9.

Prangé, R. et al. (1993), Correlated variations of UV and radio emissions during an outstanding jovian auroral event, *J. Geophys. Res.*, 98, 18,779 – 18,791.

Radioti, A. D., D. Grodent, J. C. Gérard, B. Bonfond, and J. T. Clarke (2008), Auroral polar dawn spots: Signatures of internally driven reconnection processes at Jupiter's magnetotail, *Geophys. Res. Lett.*, 35, L03104.

Saur, J., A. Pouquet, and W. H. Matthaeus (2003), An acceleration mechanism for the generation of the main auroral oval on Jupiter, Geophys. Res. Lett., 30, 1260, 319 doi:10.1029/2002GL015761.

Saur, J., Janser, S., Schreiner, A., Clark, G., Mauk, B. H., Kollmann P., et al. (2018). Wave-particle interaction of Alfvén waves in Jupiter's magnetosphere: Auroral and magnetospheric particle acceleration. Journal of Geophysical Research: Space Physics, 123, 9560–9573. https://doi.org/10.1029/2018JA025948

Szalay, J. R., Allegrini, F., Bagenal, F., Bolton, S., Clark, G., Connerney, J. E. P., et al.. (2017). Plasma measurements in the Jovian polar region with Juno/JADE. Geophysical Research Letters, 44, 7122–7130.

Szalay, J. R., Bonfond, B., Allegrini, F., Bagenal, F., Bolton, S., Clark, G., et al. (2018). In situ observations connected to the Io footprint tail aurora. Journal of Geophysical Research: Planets, 123. https://doi.org/10.1029/2018JE005752

Szalay, J. R. et al. (2020), Alfvénic acceleration sustains Ganymede's footprint tail aurora, *Geophys. Res. Lett.*, 47(3).

Thorne, R. M. et al. (1997), Galileo evidence for rapid interchange transport in the Io torus, *Geophys. Res. Lett.*., 24(17), 2131 – 2134.